Analysis of Mangrove Species Detection Performance on Multiresolution Satellite Imagery Using Linear Spectral Unmixing

Indah Fultriasanti[a,*], Aldea Noor Alina[a], Lalu Muhamad Jaelani[a], Hartanto Sanjaya[b], Abdul Rauf Abdul Rasam[c]
[a]Department of Geomatics Engineering, Institut Teknologi Sepuluh Nopember, Surabaya 60111, Indonesia
[b]Research Center for Geoinformatics, National Research and Innovation Agency (BRIN), Jakarta Pusat 10340, Indonesia
[c]College of Built Environment, Malaysia Institute of Transport, Universiti Teknologi MARA, Shah Alam, Selangor 40450, Malaysia

*Corresponding author: 6016231018@student.its.ac.id

Abstract. The Pamurbaya mangrove conservation area in East Surabaya is crucial for coastal protection, but it is vulnerable to degradation due to human activities and land-use changes. Species distribution maps are essential for understanding ecological functions, such as carbon sequestration, salinity tolerance, and ecosystem stability. This study utilizes multiresolution remote sensing data from WorldView-2 satellite imagery to map mangrove and detailed species-level. Random Forest is utilized to differentiate mangrove and non-mangrove, while Linear Spectral Unmixing allows for detailed mangrove species distribution. Further analysis was carried out to determine at what resolution the LSU works optimally. The imagery was served in 0.5 meter resolution and down-sampled to 5 meter, 10, 20, 30, and 50 meter resolutions. This study obtained that LSU were able to differentiate mangroves according to its endmember and working optimally at medium resolution (10–30 m), with overall accuracy increasing from 70% (10 m) to 75% (30 m) and Kappa value increasing from 53.7 to 60.41. High resolution (0.5–10 m) provides more detailed mapping but is optimal for species with small and scattered distributions. Meanwhile, low resolution (20–50 m) tends to cause overestimation or aggregation of species.

Keywords: Linier Spectral Unmixing; Mangrove; Mapping; Species Level; WordView-2

I. INTRODUCTION

Mangroves are group of tropical trees and shrubs that grow in the tidal zone of salt or brackish water [1]. Mangrove ecosystems have high ecological and economic value because they provide habitat for various species, protect coastlines from erosion, absorb carbon, and improve water quality [2]. Mangroves also play an important role in stabilizing sediments, dampening tsunamis, and reducing storm surges [3]. while supporting community livelihoods by increasing fish biomass and fisheries production in tropical areas [4].

Globally, the economic value of mangroves reaches 8,966–10,821 US$/ha/year. This value includes coastal protection services, fisheries habitat, carbon storage, and other ecosystem services [5] Southeast Asia has the largest mangrove ecosystem in the world[6], with Indonesia as the country with the largest mangrove forest, reaching 3.3 million hectares or 22.6 % of the world's total [7]. Papua is the region with the largest mangrove area, followed by Sumatra, Kalimantan, and other islands. The richness of mangrove species in Indonesia is very high, with 202 species recorded, including 43 species of true mangroves. In the East Coast of Surabaya (Pamurbaya) area alone, 23 species of true mangroves and 36 species of associated mangroves have been identified in 2023.

East Coast of Surabaya or Pantai Timur Surabaya (Pamurbaya), with an area of 264.87 hectares, is a protected area regulated by Surabaya Regional Regulation No. 12/2014. This area has a vital role in maintaining biodiversity and preventing activities that damage the environment [7]. However, the existence of the mangrove ecosystem in this area faces pressure due to human activities that damage the habitat, as well as the impact of climate change that threatens the sustainability of mangroves.

In response to these challenges, remote sensing technology offers an efficient, fast, and accurate solution for monitoring mangrove ecosystems [7], [8]. This method

allows detailed detection of vegetation conditions and mangrove species through satellite imagery data, which is increasingly growing with the availability of high to low resolution imagery [9]. Mangroves, with their distinctive spectral characteristics due to mud sediments and tidal water, can be identified through specific spectral responses in remote sensing imagery [10].

In this study, WorldView-2 imagery data was used because of its advantages in spatial resolution (0.5 m panchromatic, 2 m multispectral) and spectral resolution with eight bands that support detailed mapping of mangrove species distribution [11]. The Linear Spectral Unmixing (LSU) method based on spectral libraries was applied to detect mangrove species, with the uniqueness of this study in the application of LSU at various levels of WorldView-2 image resolution through down-sampling techniques up to 50-meter resolution. This downsampling technique allowed us to generate a range of image resolutions while maintaining the same spectral resolution, thereby creating a dataset with varying spatial resolutions but consistent spectral information, which enabled the evaluation of the LSU method's performance and robustness across different scales and resolutions. LSU as a sub-pixel analysis method allows species identification based on spectral characteristics [12];[13], although its application to multispectral imagery with varying resolutions is still rarely studied.

Previous studies have mostly used the LSU method on medium-resolution imagery such as Sentinel-2 through platforms such as Google Earth Engine ([7], while this study will apply LSU using the RStudio platform to analyze multiresolution imagery from WorldView-2. This study also integrates the Random Forest (RF) algorithm as an ensemble classifier that can improve the accuracy of identifying mangrove and non-mangrove areas[14]. The Random Forest machine learning classification was chosen because of its ability to handle complex datasets. Using similar training samples, Random Forest could inherently handle multi-class classification by dividing data into various categories using decision-tree-based splits [15]. Accuracy evaluation is carried out through the Confusion Matrix for RF classification and RMSE for LSU results, so that the accuracy of the method can be measured objectively.

With this approach, this study offers the advantage of exploring the performance of LSU at various resolutions of high-resolution satellite imagery, which has not been widely done prior, especially in Indonesia. This study is expected to provide a strategic contribution to mangrove conservation on the East Coast of Surabaya, as well as a scientific basis in supporting sustainable mangrove management and conservation policies.

II. METHODOLOGY

2.1 Study Area

This research focuses on the Pamurbaya area located on the coast of Surabaya City, East Java Province, Indonesia. This area is a protected area with the main function as a mangrove conservation zone and green open space, as stipulated in Surabaya City Regulation Number 12 of 2014 concerning the 2014–2034 (RTRW). The research area covers six sub-districts: Gunung Anyar, Rungkut, Sukolilo, Mulyorejo, Bulak, and Kenjeran. The research location is at coordinates 7°15’30” to 7°20’45” South Latitude and 120°47’52.52” to 120°50’47.34” East Longitude (Figure 1), making it suitable for mapping and monitoring studies on the sustainability of the mangrove ecosystem.

Figure 1. Area of Interest

2.2 Material

a) Worldview – 2

This research utilized high-resolution WorldView-2 satellite imagery, captured on February 22, 2024, with minimal cloud cover (0.001). A WorldView-2 image of the Area of Interest is presented in Figure 1. Beyond the standard four multispectral bands (blue, green, red, and near-infrared), WorldView-2 incorporates four additional bands (coastal blue, yellow, red edge, and near-infrared 2) to improve analytical capabilities. These supplementary bands are specifically intended to enhance the segmentation and classification of landuse. Key parameters of the WorldView-2 imagery in therm of spectral resolutin are also considered.

b) Mangrove Spectral Library or Endmember

Endmember can be interpreted as a pure spectral reflectance value that represents a particular object uniquely [16] This value describes the basic spectral properties of an object without being affected by external factors, such as mixing with other materials, atmospheric conditions, or other environmental effects. Due to their specific characteristics, endmembers play a very important role in various remote sensing applications, including in data analysis from satellite and hyperspectral images to identify and map objects or materials [17]. In the context of this study, endmembers are classified into four main categories, namely Avicennia marina, Rhizopora apiculata, Rhizopora mucronata, and Sonneratia alba. Data sources regarding endmember values were obtained from Badan Riset dan Inovasi Nasional (BRIN) which provide accurate references to support spectral analysis.

Spectral signature is the result of a combination of reflection, absorption, transmission, or emission of REM (Electromagnetic Radiation) by an object at various wavelengths, which allows the object to be uniquely identified. When the intensity of REM, usually expressed as reflectance in percentage form, is plotted across a range of wavelengths, the points form a curve known as the spectral signature or spectral response curve of the material. The energy reflected from an object is measured using a device called a spectrometer. Spectral reflectance data is unique to each type of material and is affected by the environmental conditions in which the measurement is made.

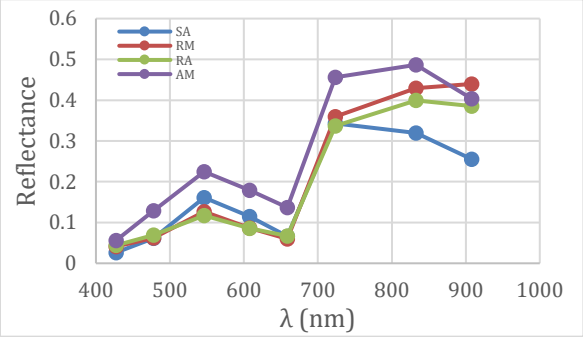

Figure 2. Spectral Endmember of Mangrove Species According to WorldView-2 Spectral Bands: Avicennia Marina (AM), Rhizopora Apiculata (RA), Rhizopora Mucronata (RM), and Sonneratia Alba (SA)

This study used reflectance values from spectral libraries provided by BRIN for mangrove species such as Avicennia marina (AM), Rhizophora apiculata (RA), Rhizophora mucronata (RM), and Sonneratia alba (SA). Endmember spectral values were obtained through measurements with an active remote sensing device, namely the Ocean Optics USB 4000+ spectrometer, which records visible light waves in the wavelength range of 200-1,100 nm. However, the spectral library used only includes endmember spectra in the wavelength range of 400-900 nm because data at wavelengths <200 nm and >900 nm are unstable.

2.3 Method

The WorldView-2 imagery underwent several preprocessing steps, including mosaicking and atmospheric correction, followed by geometric accuracy testing. The Fast Line-of-sight Atmospheric Analysis of Spectral Hypercubes (FLAASH) model was used for atmospheric correction. FLAASH based on atmospheric transmission principles, incorporates both resolution and essential atmospheric and location parameters. This process ensures that the image's spectral values represent Bottom of Atmosphere reflectance, making them more appropriate for land use classification [18].

Geometric accuracy testing revealed an error of less than 4.5 m (specifically, 4.421 m). This result indicates that the WorldView-2 imagery meets the accuracy standards for 1:5,000 scale Class 2 level mapping, as defined by Indonesian National Standard 8202-2019 for Base Map Accuracy.

Pansharpening was applied to enhance the spatial resolution of the multispectral imagery, changing the cell size from 2 m to 0.5 m to match the resolution of the panchromatic band.

The Random Forest algorithm was employed to distinguish mangrove areas from other land uses, including ponds, water bodies, and built-up areas. The performance of the classification was then evaluated using a confusion matrix to determine the accuracy. Mangrove coverage resulted from random forest classification then used as an further Area of Interest. This means that Linear Spectral Unmixing (LSU) will later be clipped in this mangrove coverage.

The determination of endmembers in this study is based on the reflectance values representing each mangrove species, namely Avicennia marina, Rhizophora apiculata, Rhizophora mucronata, and Sonneratia alba. The spectral values of each endmember were separated following the wavelength range of the channel in the WorldView-2 image. Then, a representative value representing the middle wavelength for each channel is selected for each endmember.

The spectrum obtained from the endmember is then used as a parameter in the LSU processing process.
LSU is used to estimate the proportion of spectral components of each image pixel. The Fully Constrained LSU algorithm is chosen because the value of the sum of endmember abundances must be equal to 1 and the abundance value must not be less than zero.

Linear Spectral Unmixing (LSU) assumes that the endmember abundances in mixed pixels can be described using a linear model, which makes it easy to use due to its simple calculation. Equation (1) is the formula for LSU. However, the drawback is that this model does not take into account possible interactions between objects that can be detected by satellite sensors.

$$R_k = \sum_{i=1}^{n} r_{i,k}.\, a_i + \varepsilon_k \qquad (1)$$

R is the reflectance value of the mixed pixel, r is the reflectance value of the endmember, a is the total of the endmembers, ε is the error value, k is the number of satellite channels, and i is the number of endmembers. There is a limit to the number of endmembers. The ideal maximum number is k-1, which is lower than the number of satellite channels. [19]. The following is the matrix equation resulting from the LSU formula calculation:

$$\begin{bmatrix} R_1 \\ R_2 \\ R_3 \\ R_4 \\ R_5 \\ R_6 \\ R_7 \\ R_8 \end{bmatrix} = \begin{bmatrix} r_{1,1} & r_{1,2} & r_{1,3} & r_{1,4} \\ r_{2,1} & r_{2,2} & r_{2,3} & r_{2,4} \\ r_{3,1} & r_{3,2} & r_{3,3} & r_{3,4} \\ r_{4,1} & r_{4,2} & r_{4,3} & r_{4,4} \\ r_{5,1} & r_{5,2} & r_{5,3} & r_{5,4} \\ r_{6,1} & r_{6,2} & r_{6,3} & r_{6,4} \\ r_{7,1} & r_{7,2} & r_{7,3} & r_{7,4} \\ r_{8,1} & r_{8,2} & r_{8,3} & r_{8,4} \end{bmatrix} \times \begin{bmatrix} a_1 \\ a_2 \\ a_3 \\ a_4 \end{bmatrix} + \begin{bmatrix} \varepsilon_1 \\ \varepsilon_2 \\ \varepsilon_3 \\ \varepsilon_4 \\ \varepsilon_5 \\ \varepsilon_6 \\ \varepsilon_7 \\ \varepsilon_8 \end{bmatrix} \qquad (2)$$

Linear Spectral Unmixing (LSU) analysis with 8 bands and 4 endmembers (SA, AM, RA, and RM) can be represented in matrix form. In this process, the reflectance in each band R is calculated as a linear combination of the spectral reflectance of each endmember E multiplied by the abundance value A of each endmember, plus the error component ε. The endmember spectral matrix E has dimensions of 8x4, where each row shows the reflectance value of each band (B1 to B8), and each column represents the endmember (SA, AM, RA, and RM). Meanwhile, the abundance vector A contains the proportion of each endmember whose value meets the physical requirements, namely non-negative and has a total of 1.

LSU utilizes the equation R=E·A+ε, which describes that the reflectance value in each band Rk is the result of multiplying the spectral matrix of endmember E by the abundance vector A, plus the noise or error component εk. This method allows the spectral separation of each image pixel into the contributions of each endmember, so that it can be used to identify and map the distribution of mangrove vegetation or other objects based on their spectral characteristics.

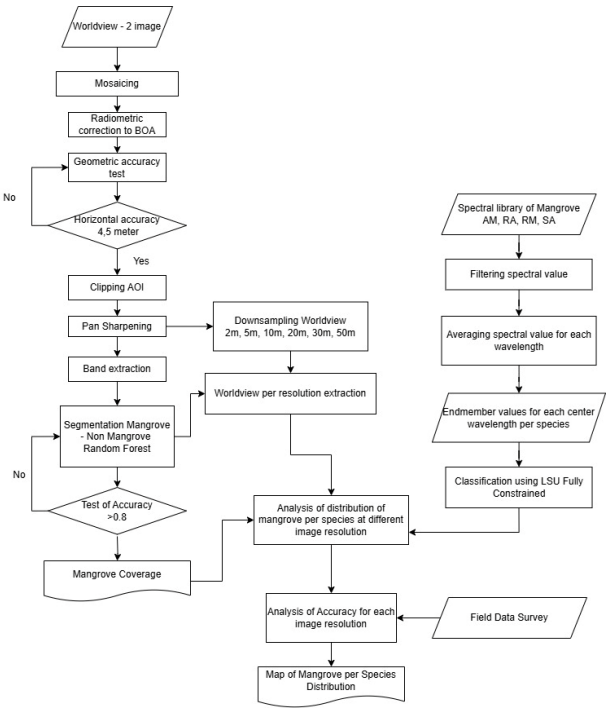

Figure 3. Research Flow Method

2.4. Root Mean Squared Error (RMSE)

Knowing the error value of the LSU (Linear Spectral Unmixing) method can be evaluated by calculating the Root Mean Squared Error (RMSE). Root Mean Square Error (RMSE) is an important metric for evaluating the accuracy of Linear Spectral Unmixing (LSU) results in remote sensing analysis, one of which is Root Mean Square Error (RMSE) is used as an indicator to assess the accuracy of Linear Spectral Unmixing (LSU) results by comparing the abundance map of LSU results (prediction) and the reference map or ground truth. RMSE is calculated based on the average squared difference between the predicted value and the reference value, which is then rooted to return the unit to the initial scale. The RMSE formula can be written as follows:

$$RMSE = \sqrt{\frac{\sum_{i=1}^{N} \|y(i) - \hat{y}(i)\|^2}{N}} \qquad (3)$$

Where y(i) is the reference value or ground truth at pixel i, y̑(i) is the predicted value of the LSU result at pixel i, and N is the total number of pixels. In the context of LSU, the abundance map shows the fractional distribution of endmembers in mangrove species in each image pixel. The RMSE value provides a measure of the average error between the LSU prediction results and the reference data. In this study, the RMSE value ≤ 0.5 is used, which is expected to result from processing using the LSU (Linear Spectral Unmixing) method can be said to be accurate or close to the actual value.

The RMSE threshold value ≤ 0.5 is often used in remote sensing analysis as an indicator of acceptable error, especially in Linear Spectral Unmixing (LSU) applications. The basis for using this threshold is that the RMSE value reflects the average deviation of the model results compared to the reference value (ground truth). In LSU, the abundance value is calculated as a fractional proportion between 0 and 1, so that the average error ≤ 0.5 indicates a maximum deviation of 50% from the full scale, which is considered low enough to ensure the accuracy of the results. According to the study [20] entitled Thematic Map Comparison: Evaluating the Statistical Significance of Differences in Classification Accuracy, states that a small RMSE value indicates that the classification error on the thematic map is still within the tolerance limit. Meanwhile, Roberts et al. [21] with their research entitled Mapping Chaparral in the Santa Monica Mountains Using Multiple Endmember Spectral Mixture Models, also emphasized that RMSE is used to evaluate fractional distribution in Multiple Endmember Spectral Mixture Analysis (MESMA) analysis, and a value of ≤ 0.5 reflects a good representation of the reality in the field. Therefore, in the context of mangrove mapping, RMSE ≤ 0.5 is relevant to indicate that the abundance prediction from the LSU model is accurate enough to be used in further analysis, although this value can be adjusted based on research needs.

Field measurements were conducted to test the accuracy of LSU processing results in determining each type of mangrove. The results of mangrove distribution per type will be compared with actual conditions in the field. This accuracy test was conducted for each image resolution to determine the level of accuracy of LSU results at different image resolutions.

2.5. Classification Accuracy Assessment

In this study, validation testing was conducted on the results of image classification which included the combination of several types of mangrove species, namely Avicennia Marina, Rhizophora Apiculata, Rhizophora Mucronata, and Sonneratia Alba. The purpose of this classification accuracy test is to identify potential classification errors and calculate the percentage of the resulting accuracy level. The method used involves creating a contingency matrix, often referred to as a confusion matrix, to evaluate the classification results. This confusion matrix is a tool commonly used to assess the performance of classification models, especially in machine learning[22]. The matrix describes the number of correct and incorrect predictions from the model, which is formulated based on the approach of Short [23] , with the following equation.

$$MA = \frac{(X_{cr\ pixel})}{(X_{cr\ pixel} + X_{o\ pixel} + X_{co\ pixel})} \times 100\% \quad (4)$$

MA = *Mapping accuracy*
Xcr = Corrected X value
Xo = Number of class X students who entered another class (omission)
Xco = Number of additional class X from other classes (commission)

Omission error occurs when pixels that should be included in a class are instead classified into another class, so that the number of pixels in the original class is reduced. Evaluation of classification accuracy can be done with several metrics, such as overall accuracy, producer's accuracy, user's accuracy, and kappa index. The formula for calculating each of these indicators refers to [24] as follows.

a. Overal Accuracy
   Overall accuracy is often used because it considers all elements in the contingency matrix to evaluate classification accuracy. This makes it able to provide a more comprehensive assessment than overall accuracy, which only focuses on correctly classified pixels. The formula for calculating Kappa Accuracy is as follows:

$$Overall\ Accuracy = \frac{D}{N} \times 100\% \quad (5)$$

   D = Number of correct row values that have been added diagonally
   N = Number of correct values in the error matrix

b. Producer's Accuracy
   Producer's Accuracy shows the average probability (%) of a pixel being correctly classified. This indicates how well each class in the field is classified. A producer's accuracy value of 100% for all classes

indicates that no pixels from that class were classified into any other class. Here is the formula for calculating producer's accuracy:

$$Producer's\ Accuracy = \frac{X_{ii}}{X_{+i}} \times 100\% \qquad (6)$$

X_ii= Number of correct cell values in class
X_(+i)= Number of cell values in column i

c. User'Accuracy
User's Accuracy shows the average probability (%) that a pixel from a classified image truly represents its class in the field. This shows how well the classification model is in identifying different classes. A User's Accuracy value of 100% for all classes indicates that there is no misclassification, where the model does not take pixels from other classes. Here is the formula for calculating User's Accuracy:

$$User's\ Accuracy = \frac{X_{ii}}{X_{i+}} \times 100\% \qquad (7)$$

Xii= Number of correct cell values in class
X(i+)= Number of cell values in row i

d. Kappa Accuracy
Kappa accuracy is often used because it calculates classification accuracy by involving all elements in the contingency matrix. This approach provides a more in-depth evaluation compared to overall accuracy, which only considers the number of correctly classified pixels. Here is the formula for calculating Kappa Accuracy:

$$Kappa\ Accuracy = \frac{\sum_{i=1}^{r} X_{ii} - \sum_{i=1}^{r}(X_i \times X_{+i})}{N^2 - \sum_{i=1}^{r}(X_i \times X_{+i})} \qquad (8)$$

r = Row number in the matrix
X_ii= Number of correct cell values in class
X_(i+)= Number of cell values in row i
X_(+i)= Number of cell values in column i
N = Number of cell numbers in the error matrix

III. RESULT AND DISCUSSION

3.1 LSU Results for Avicennia Marina, Rhizophora Apiculata, Rhizophora Mucronata, and Sonneratia Alba at All Resolutions

The abundance map generated through the spectral unmixing algorithm using R Studio depicts the relative abundance value based on the spectral model for each pixel. The abundance value on this map does not always represent the percentage of endmembers on a scale of 0-1 or 0-100%, as explained by previous researchers [7]). The higher the percentage of objects in a land or pixel, the closer the abundance value will be to 1. Conversely, the lower the percentage, the smaller the presence of the object [25]. The results of this processing obtained an abundance map displayed in Figures 4.4 to 4.7, which shows the spatial distribution of mangrove species A. Marina, R. Apiculata, R. Mucronata, and S. Alba in the East Coast Protected Area of Surabaya. These results show that the green color on the map indicates areas with higher abundance, while the red color indicates areas with lower abundance. The results in the form of abundance maps for each mangrove species at various levels of resolution provide an overview of the spatial distribution, which will be described in the following explanation.

a. Distribution of Mangrove Species Avicennia Marina

The distribution results of the mangrove species Avicennia marina with a range of values 0 to 100%. Green color indicates the percentage of LSU of 70-100%, yellow color indicates the percentage of 50-70%, orange color indicates the percentage of 30-50%, and red color indicates the percentage of 0-30%. The results of the LSU analysis at various levels of resolution show that the A. marina species is mostly in the range of 70-100% (marked in green), which indicates the high abundance and dominance of this species in each pixel. In addition, the percentage of 50-70% (yellow color) is also classified as the second dominant in its distribution area in all LSU results at all levels of resolution, namely 0.5m, 2m, 5m, 10m, 20m, 30m, and 50m. Distribution with a percentage range of 30-50% (orange color) and 0-30% (red color) was found only in a few areas.

Based on LSU analysis, A. marina dominates the Pamurbaya protected area and is widely found in the Gunung Anyar Mangrove Botanical Garden and Wonorejo, especially with a percentage range of 50 - 100% at all levels of resolution. This species is the most common type of mangrove found in tidal areas and is known as a pioneer in protected coastal areas. With high tolerance to salinity levels, A. marina is able to grow well in fluctuating environments.

The existence of this species plays an important role in preventing coastal abrasion and increasing the stability of the mangrove ecosystem. Its respiratory roots function to oxygenate the soil and support the lives of various organisms around it. Its wide distribution and dominance reflect its good adaptability to various mangrove ecosystem conditions in the research area. The following are the results of the distribution of the Avicennia marina mangrove species at each image resolution level, namely 0.5 m, 2 m, 5 m, 10 m, 20 m, 30 m, and 50 m.

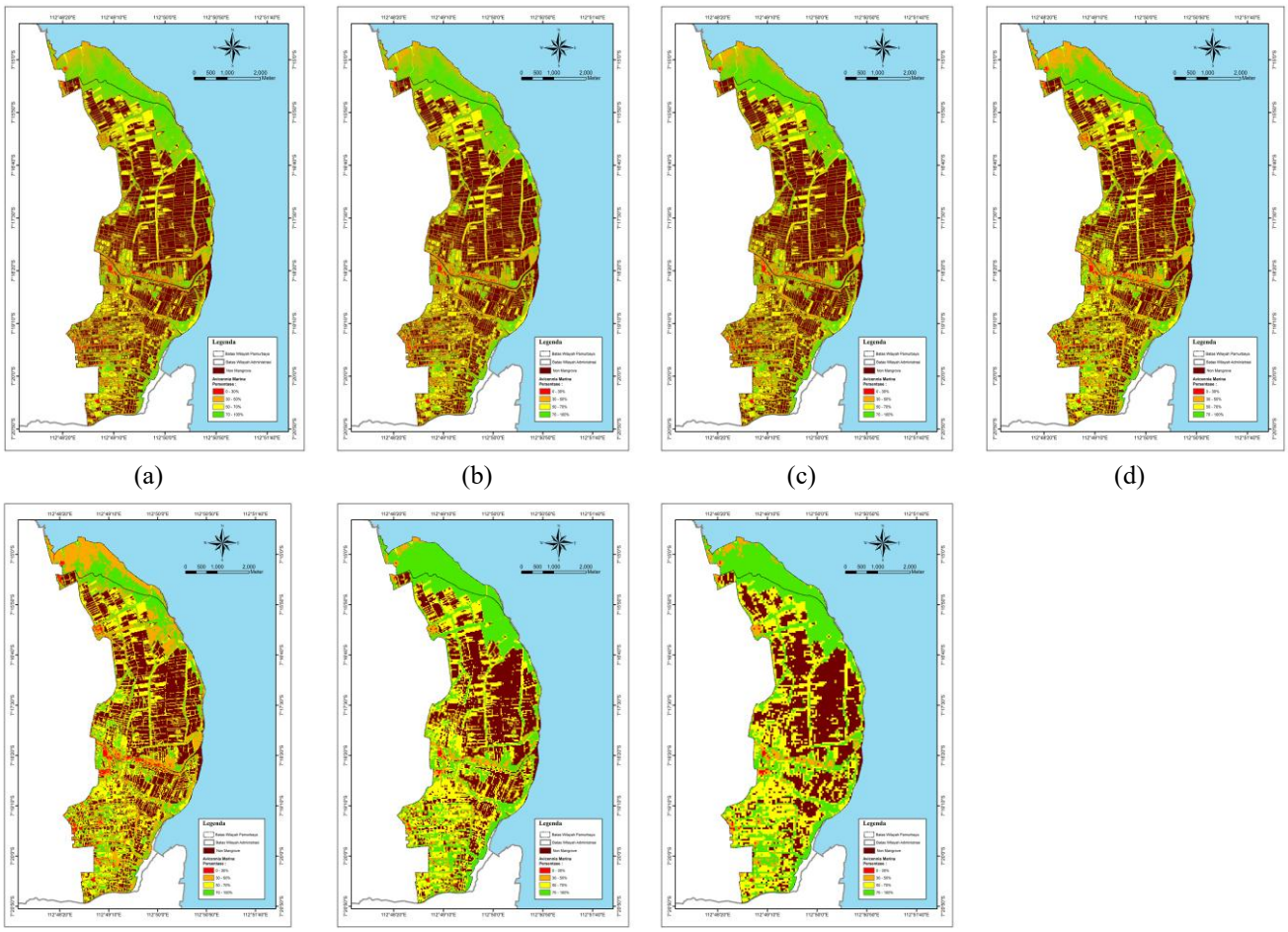

(a) (b) (c) (d)

(e) (f) (g)

Figure 4. Classification Results of Avicennia marina Mangrove Species using LSU Processing at Multiple Spatial Resolution Levels
(a) 0.5m, (b) 2m, (c) 5m, (d) 10m, (e) 20m, (f) 30m, (g) 50m

b. Distribution of Mangrove Species Rhizopora Apiculata

The distribution results of the mangrove species Rhizopora Apiculata at each resolution level in Figure 4.5 show a range of 0 to 100%. The green color indicates the percentage of LSU of 70 - 100%, the yellow color indicates the percentage of 50 - 70%, while the orange to red colors indicate the percentage of 0 - 50%. Based on the results of the LSU analysis, the distribution of Rhizophora apiculata shows a varied distribution pattern at different spatial resolutions. At high resolution (0.5m to 5m), the spatial distribution of R. apiculata looks more detailed, with dominance centered in the middle mangrove zone or indicated by the green color. This area tends to have environmental conditions that support the growth of R. Apiculata, such as optimal salinity levels and the presence of mud substrates. Conversely, at medium to low resolution (10m to 50m), the distribution pattern looks more homogeneous due to the pixel generalization effect, so that areas with low dominance and a mixture of other species are more difficult to distinguish. Overall, most of the Pamurbaya Protected Area shows a distribution percentage of R. apiculata in the range of 50 - 70%, indicating the presence of other more dominant mangrove species, such as Avicennia marina. Only a small part of the Pamurbaya area has a range of 70-100% for the R. Apiculata species.

There are several factors that influence the R. Apiculata species not to dominate the Pamurbaya area. Factors such as salinity fluctuations, soil conditions, and resource competition with other species also

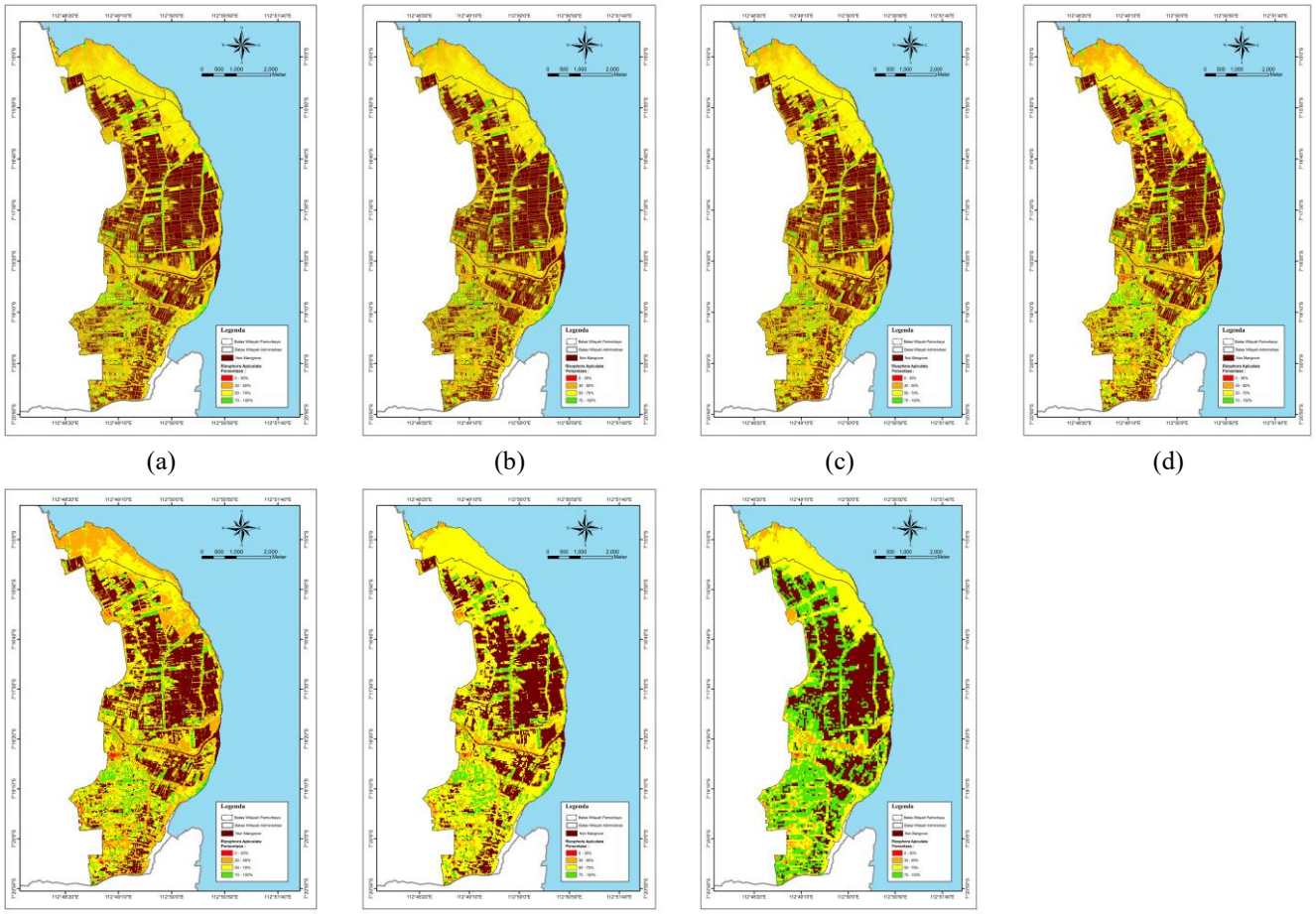

(a) (b) (c) (d)

(e) (f) (g)

Figure 5. Classification Results of Rhizopora apiculata Mangrove Species using LSU Processing at Multiple Spatial Resolution Levels (a) 0.5m, (b) 2m, (c) 5m, (d) 10m, (e) 20m, (f) 30m, (g) 50m

influence the distribution of R. apiculata. This species is optimal in the middle mangrove zone, but does not dominate completely due to ecological variations in the area. In the Pamurbaya area, there are several other mangrove species that also have tolerance to harsh environmental conditions. These species, such as Avicennia Marina, can compete with R. Apiculata for resources such as water, light, and nutrients. This competition can limit the ability of R. Apiculata to dominate the area [7]. The following is the distribution of the Rhizopora Apiculata mangrove species at each image resolution level, namely 0.5 m, 2 m, 5 m, 10 m, 20 m, 30 m, and 50 m.

c. Distribution of Mangrove Species Rhizopora Mucronata

The results of the distribution of the mangrove species Rhizopora Mucronata can be seen in Figure 4.6, which shows a range of 0 to 100%. The green color indicates the percentage of LSU of 70 - 100%, the yellow color indicates a percentage of 50 - 70%, while the orange to red colors indicate a percentage of 0 - 50%.

In the results of this LSU analysis, it shows a few areas with a percentage value of 50-70% which reflects high dominance by R. Mucronata, where most of the spectral in the pixel comes from this species, indicating optimal habitat, in the Wonorejo Mangrove Botanical Garden and Gunung Anyar areas. This species grows naturally and is often planted in the area, especially in the middle mangrove zone with mud substrates that support its growth. Conversely, areas with a percentage value of 0-50% indicate that in 1 pixel there is a mixture of other mangrove species that are more dominant than R. Mucronata, usually found in the transition zone or open mangrove zone.At high resolution (0.5m to 5m), the distribution of R.

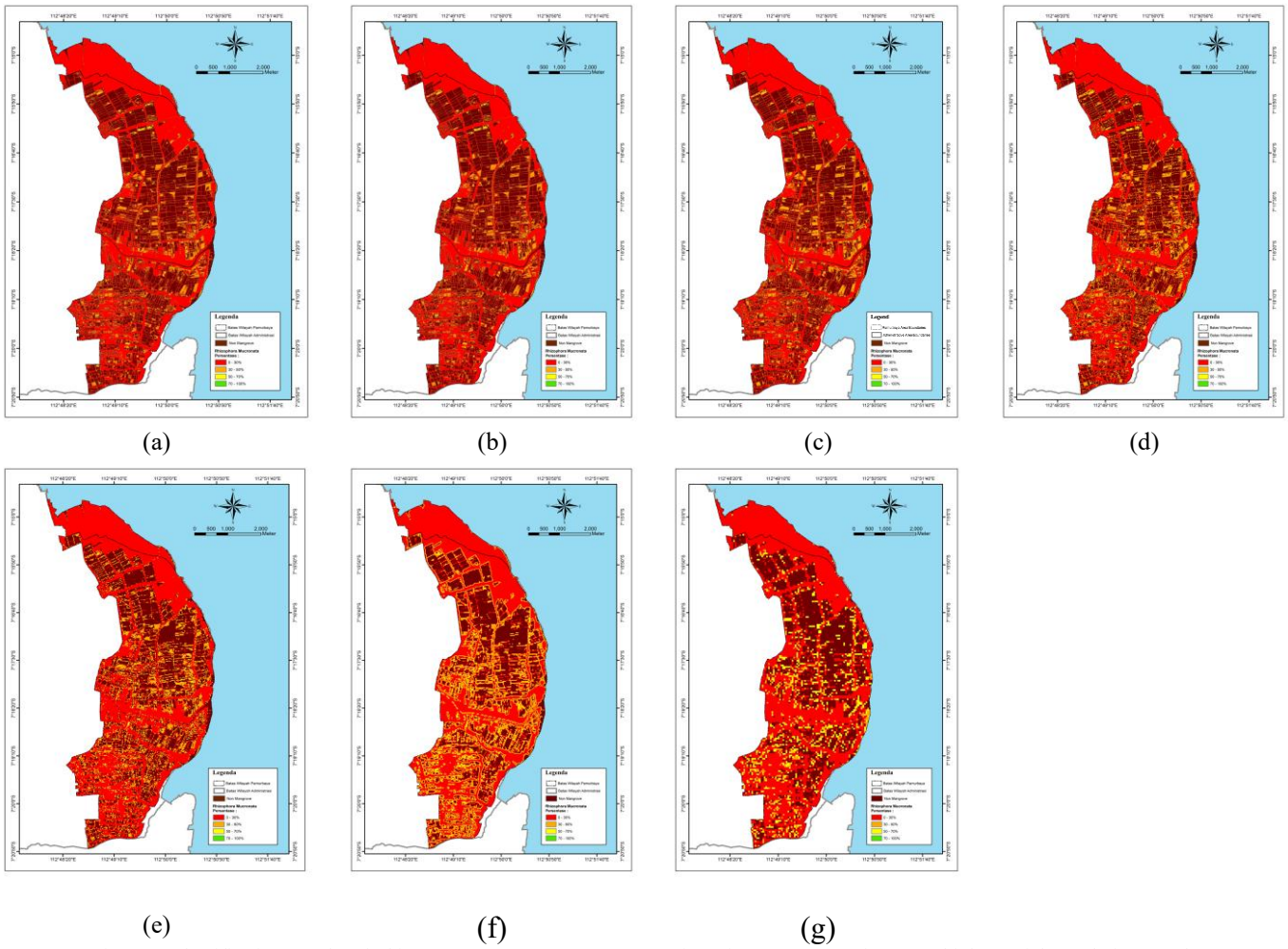

Figure 6. Classification Results of Rhizopora mucronata Mangrove Species using LSU Processing at Multiple Spatial Resolution Levels (a) 0.5m, (b) 2m, (c) 5m, (d) 10m, (e) 20m, (f) 30m, (g) 50m

Mucronata looks more detailed, while at medium to low resolution (10m to 50m), the distribution pattern tends to be more homogeneous due to pixel generalization, making mixed species more difficult to distinguish. The following is the distribution of Rhizopora mucronata mangrove species at each image resolution level, namely 0.5 m, 2 m, 5 m, 10 m, 20 m, 30 m, and 50 m.

d. Distribution of Mangrove Species Sonneratia Alba

The distribution results of the mangrove species Sonneratia Alba can be seen in Figure 4.7, which shows a range of 0 to 100%. The green color indicates the percentage of LSU of 70 - 100%, the yellow color indicates a percentage of 50 - 70%, while the orange to red colors indicate a percentage of 0 - 50%. Based on the LSU analysis at various levels of resolution, it is known that most of the Pamurbaya area has a low percentage of S. alba, which is around 0-30%. This confirms that this species has not yet dominated the protected area of the East Coast of Surabaya. Research by [7] stated that in the Wonorejo Mangrove Botanical Garden, this species is still widely planted in pots or polybags and is not evenly distributed throughout the Pamurbaya area, in contrast to species such as Avicennia marina, Rhizophora apiculata, and Rhizophora mucronata. This low percentage also indicates that in one pixel there is a mixture with other mangrove species. As additional information, the 2019 mangrove density study report noted that S. alba dominates several areas on the East Coast of Surabaya (Panturbaya), because this species has the ability to grow well in sandy, rocky, or coral reef habitats. Ecologically, S. Alba makes an important contribution to the environment, such as supporting high biodiversity by being a nursery for various species of fish and crustaceans. Research by [7] stated that in the Wonorejo Mangrove Botanical Garden, this species is still

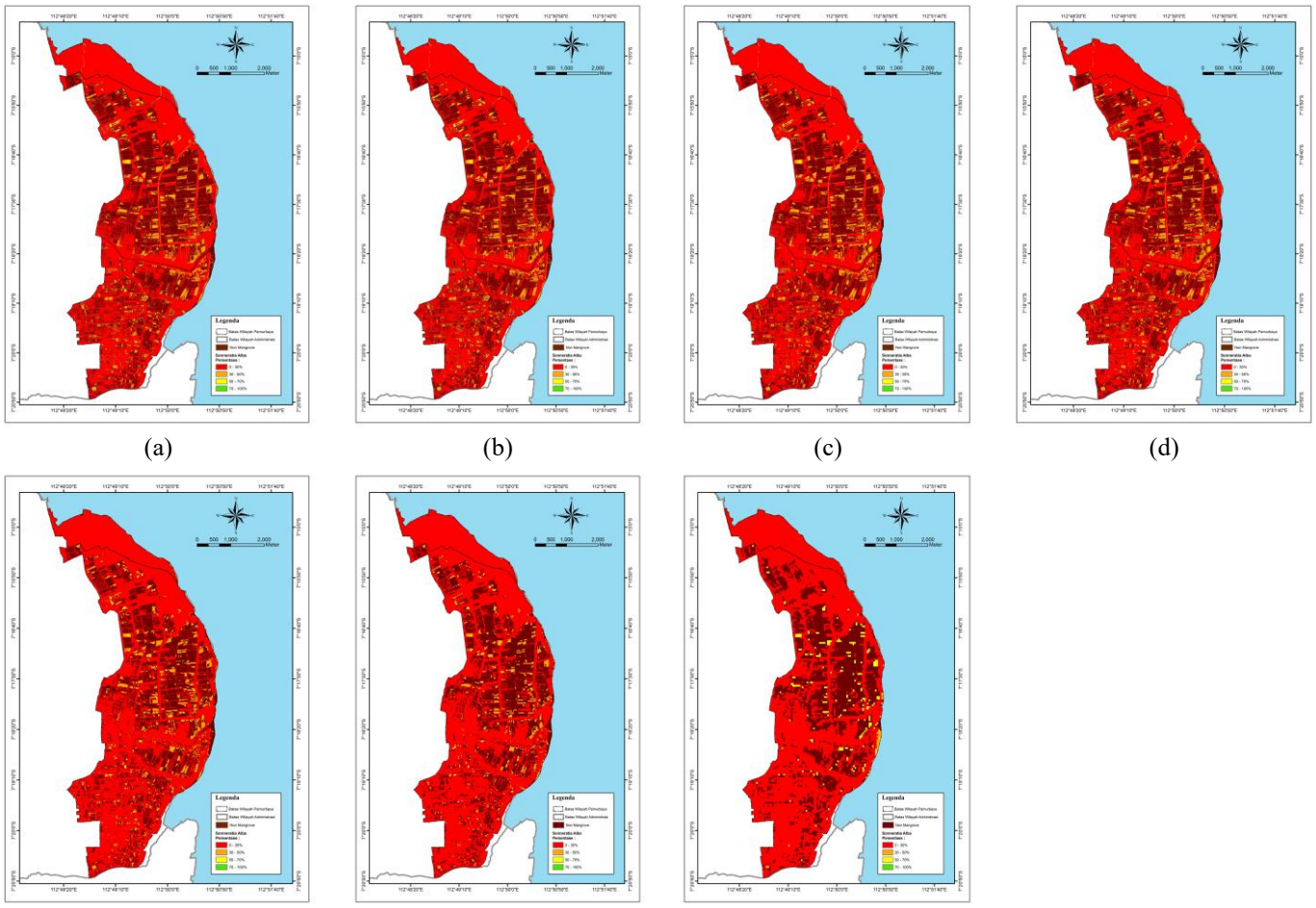

Figure 7. Classification Results of Sonneratia alba Mangrove Species using LSU Processing at Multiple Spatial Resolution Levels
(a) 0.5m, (b) 2m, (c) 5m, (d) 10m, (e) 20m, (f) 30m, (g) 50m

widely planted in pots or polybags and is not evenly distributed throughout the Pamurbaya area, in contrast to species such as Avicennia marina, Rhizophora apiculata, and Rhizophora mucronata. This low percentage also indicates that in one pixel there is a mixture with other mangrove species. As additional information, the 2019 mangrove density study report noted that S. alba dominates several areas on the East Coast of Surabaya (Panturbaya), because this species has the ability to grow well in sandy, rocky, or coral reef habitats. Ecologically, S. Alba makes an important contribution to the environment, such as supporting high biodiversity by being a nursery for various species of fish and crustaceans. In addition, S. alba roots play a role in filtering pollutants and binding sediments, thereby helping to improve water quality and protecting coral reefs and seagrass from sedimentation by [6]. Due to its great benefits, it is hoped that in the future the Pamurbaya area can expand the planting of S. alba massively in protected areas. The distribution of Rhizopora Mucronata mangrove species at each image resolution level, namely 0.5 m, 2 m, 5 m, 10 m, 20 m, 30 m, and 50 m is presented in Figure 7.

3.2. Comparison of Mangrove Species Area from LSU Processing at Different Image Resolutions

The results of the LSU processing analysis show that the area of mangrove species varies depending on the image resolution used. Avicennia Marina tends to increase in area with increasing image resolution, from 70.18918 km² at 0.5 meter resolution to 70.9675 km² at 50 meter resolution, although the percentage of cover decreases slightly from 37.46% to 36.94%. This indicates that coarse resolution has the potential to cause overestimation of this

species. Meanwhile, Rhizophora Apiculata experienced a more significant increase in area from 51.34974 km² at 0.5 meter resolution to 56.97 km² at 50 meter resolution, with the percentage of cover increasing from 27.39% to 29.66%. This increase is more visible at 5 meter resolution and above, indicating the possibility of class merging with other species that have similar spectral. For Rhizophora Mucronata, the area fluctuates, with the lowest value at 10-meter resolution of 33.1012 km² and the highest at 50-meter resolution of 40.365 km². At high resolution (0.5 - 5 m), the area is relatively stable, while at coarse resolution (20 - 50 m), the area increases quite significantly, indicating the possibility of misclassification with other species, especially Rhizophora Apiculata. Meanwhile, Sonneratia Alba actually experienced a decrease in area from 29.20018 km² at 0.5-meter resolution to 23.7675 km² at 50-meter resolution, with the percentage of cover also decreasing from 15.58% to 12.38%. This decrease indicates that coarse resolution cannot capture this species well, possibly because its distribution is more widespread and less dominant than other species.

Overall, the mangrove area is dominated by Avicennia marina with the highest area of 70.97 km² (36.94%) at 50-meter resolution, and shows a relatively stable distribution at all resolutions (0.5–50 m). Rhizophora apiculata is in second place with an area of 56.97 km² (29.66%) at 50-meter resolution, showing an increasing trend in area as pixel size increases. Furthermore, Rhizophora mucronata has a maximum area of 40.37 km² (21.02%) at 50-meter resolution, although it experienced a decrease at medium resolution. Sonneratia alba is the species with the smallest area of 23.77 km² (12.38%) at 50-meter resolution, and is most affected by changes in resolution, especially in images with coarse pixels.

Image resolution significantly affects the results of LSU processing, especially in detecting the area of mangrove species. Avicennia Marina and Rhizophora Apiculata experienced an increase in area with increasing resolution, while Rhizophora Mucronata showed a fluctuating trend indicating high sensitivity to changes in resolution. On the other hand, Sonneratia Alba experienced a decrease in area indicating that coarse resolution could not capture this species well. Therefore, the selection of resolution in LSU analysis needs to be adjusted to the research objectives, whether prioritizing spatial accuracy or wider area coverage.

The following is a comparison of the area of LSU processing at various levels of image resolution for each mangrove species in the Pamurbaya area.

3.2. LSU Spectral RMSE Results

The results of the RMSE analysis of the LSU abundance map show that the level of classification accuracy varies for each mangrove species analyzed. The RMSE value provides a measure of the average error between the LSU prediction results and the reference data, which indicates how well the LSU method is in classifying the distribution of mangrove species fractionally in each image pixel. In this study, the RMSE threshold value ≤ 0.5 was used as the acceptable accuracy limit. This value is often used in remote sensing analysis as an indicator of the level of error that can still be tolerated, especially in Linear Spectral Unmixing (LSU) applications. From the analysis results, Rhizophora apiculata (RA) and Rhizophora Mucronata (RM) showed low RMSE values, ranging from 0.085 - 0.102 for RA and 0.104 - 0.116 for RM, respectively. This value is far below the threshold of 0.5, indicating that the LSU method can identify the distribution of these species well and the level of classification error is very small. Avicennia Marina (AM) has a higher RMSE value, ranging from 0.227 – 0.239, but is still in the accurate category because it is still below the threshold of 0.5.

Table 1. Area per Species Generated from LSU Processing at Various Levels of Image Resolution

No	Image Resolution (m)	Mangrove Species							
		Avicennia Marina		Rhizophora Apiculata		Rhizophora Mucronata		Sonneratia Alba	
		km²	%	km²	%	km²	%	km²	%
1	0.5	70.189	37.46	51.350	27.39	36.697	19.57	29.200	15.58
2	2	70.199	37.46	51.354	27.39	36.707	19.58	29.201	15.57
3	5	70.236	37.28	52.391	27.81	35.937	19.08	29.8161	15.83
4	10	70.339	37.22	53.094	28.11	33.101	17.53	32.3711	17.14
5	20	70.508	36.94	55.336	28.98	35.632	18.66	29.4571	15.42
6	30	70.668	36.91	56.076	29.27	37.919	19.79	26.8701	14.03
7	50	70.968	36.94	56.970	29.66	40.365	21.02	23.768	12.3

This can be attributed to the dominance of this species in the study location, which makes its reflectance variation greater due to differences in vegetation density and environmental conditions.

In contrast, Sonneratia Alba (SA) has the highest RMSE value, which is between 0.557 - 0.593, which means that this value exceeds the threshold of 0.5. This indicates that the LSU method is less accurate in identifying the distribution of SA. Based on the results of field observations, SA is still in the growth stage, so its reflectance is more difficult to distinguish from the surrounding soil or water substrate. This factor causes LSU to have difficulty in determining the fractional proportion of this species accurately, thereby increasing the level of classification errors.

In the context of LSU, the abundance map shows the fractional distribution of endmembers in mangrove species in each image pixel. The error measured through the RMSE value represents the deviation between the model results and the reference value (ground truth). With an RMSE value ≤ 0.5, the classification error is still acceptable because the maximum deviation that occurs is only 50% of the full scale (0 to 1). Based on the calculation, the average RMSE value at all levels of image resolution is obtained as follows: Avicennia marina is 0.227, Rhizophora apiculata is 0.093, Rhizophora mucronata is 0.107, and Sonneratia alba is 0.574. Thus, the LSU method used has shown good performance in mapping the distribution of mangrove species, except for species that are still in the growth stage such as SA, which require more attention in endmember selection and additional validation using field data.

The RMSE value in LSU analysis is influenced by the level of image resolution, which is closely related to how dominant a mangrove species is in the field. More dominant species tend to have a wide and uniform distribution, so that LSU can identify the fraction of these species more accurately. For example, Avicennia marina which has a wide coverage shows a relatively low RMSE value even though the image resolution decreases. This is due to its dominant presence, reducing the possibility of spectral mixing with other species or backgrounds such as water and soil. In addition, the level of image resolution also plays a role in determining the level of spectral mixing. At higher resolutions, such as 0.5 m, each pixel represents a smaller area, so the possibility of covering only one type of species is greater. This reduces the effect of spectral mixing and decreases the RMSE value. Conversely, at lower resolutions, such as 50 m, one pixel can cover several species simultaneously, increasing classification errors and RMSE values, especially for species with non-uniform distributions.

Other factors that affect the RMSE value are the condition of the species and its reflectance. Species that are still in the growth stage, such as Sonneratia alba in this study, are more difficult to classify because their reflectance can mix with substrates such as soil or water. LSU has difficulty in accurately identifying species fractions, so the RMSE value tends to be higher, especially at lower resolutions. Thus, dominant and evenly distributed species, such as Avicennia marina and Rhizophora apiculata, tend to have more stable and low RMSE values at various resolutions. Conversely, species with smaller coverage or uneven distribution, such as Sonneratia alba, show an increase in RMSE values at lower resolutions. This confirms that the RMSE value in LSU is greatly influenced by image resolution and species dominance in the field.

To improve the accuracy of LSU results, several steps that can be taken include selecting more optimal endmembers to avoid overlap between species with similar reflectance, increasing image resolution because higher resolution (e.g. 0.5m – 5m) can reduce spectral mixing and produce lower RMSE, and validation with field data especially for species that have high RMSE values such as SA so that LSU classification is more accurate. By considering these factors, LSU abundance mapping can be further improved, so that the distribution of mangrove species can be represented more accurately and can be used effectively in ecological studies and mangrove ecosystem management.

Table 2. RMSE per Species at Various Levels of Image Resolution

No	Resolution (m)	RMSE			
		AM	RA	RM	SA
1	0.5	0.231	0.102	0.104	0.557
2	2	0.230	0.102	0.104	0.558
3	5	0.229	0.099	0.104	0.561
4	10	0.227	0.093	0.106	0.575
5	20	0.225	0.088	0.109	0.584
6	30	0.223	0.086	0.110	0.587
7	50	0.221	0.083	0.112	0.593

3.3. Mangrove Species Accuracy Assessment

Based on the results of the accuracy test of mangrove species types carried out at resolution levels of 0.5 m, 2 m, 5 m, 10 m, 20 m, 30 m and 50 m. which is calculated using a confusion matrix shows an increase in overall accuracy along with increasing pixel resolution. At a resolution of 0.5 m, the overall accuracy reaches 59.16% with a Kappa value of 43.19, indicating a moderate level of agreement between the classification and reference data. Along with

increasing pixel resolution up to 5 m, the accuracy increases gradually with overall accuracy reaching 65.84% and a Kappa value of 50.45, indicating improvements in mangrove class mapping. The most significant increase is seen at a resolution of 10 to 30 m, where overall accuracy increases from 70% at a resolution of 10 m to 75% at a resolution of 30 m, with a Kappa value increasing to 60.41. At a resolution of 50 m, overall accuracy decreases slightly to 74.16%, and the Kappa value reaches 57.43.

In general, user accuracy and producer accuracy show an increasing trend for the Avicennia Marina and Rhizophora Apiculata classes, while the Sonneratia Alba class has lower accuracy at all resolutions. This indicates that higher image resolutions produce more accurate classifications for certain mangrove species, although at resolutions that are too high such as 0.5 m, there is a possibility of overfitting or inaccuracy due to spectral variations within one mangrove class.

The LSU results show quite good performance at medium resolutions, namely between 10 and 30 m. In this resolution range, the overall accuracy increases from 70% (10 m) to 75% (30 m), and the Kappa value also increases from 53.7 to 60.41, indicating a better level of agreement between the classification and the reference data. In addition, user accuracy and producer accuracy for most mangrove classes also tend to be more stable compared to higher resolutions (0.5–5 m), which are likely to experience overfitting or greater spectral variations within one class. Thus, medium resolution (10–30 m) can be considered a good compromise between classification accuracy and processing efficiency, especially if the main goal is large-scale mangrove mapping without losing too much species-specific detail.

At 50-meter resolution, LSU results tend to be less than optimal for identifying certain types of mangroves that have a small scale or are spread over a more limited area. This resolution is more suitable for mapping large areas of mangroves and identifying dominant species, but is less accurate in distinguishing more varied species on a small scale. This can be seen from the overall accuracy which decreased slightly to 74.16%, and the Kappa value which reached 57.43, lower than medium resolution (10–30 m). In addition, user accuracy and producer accuracy in several classes, especially Sonneratia Alba, decreased significantly, indicating that mangrove types with smaller distributions are difficult to detect properly at low resolution. Thus, 50-meter resolution is more suitable for land cover change analysis or general mangrove mapping, but is less ideal for studies that require more detailed and accurate identification of mangrove species. The following are the accuracy values of LSU processing at various levels of image resolution for each mangrove species in the Pamurbaya area.

Table 3. Accuracy Assessment at 0.5m Resolution

Class	*AM*	*RA*	*RM*	*SA*	*T*	*U*	*O*	*K*
AM	34	15	16	14	79	43.03	0	0
RA	0	16	3	0	19	84.21	0	0
RM	0	1	18	0	19	94.73	0	0
SA	0	0	0	3	3	100	0	0
T	34	32	37	17	120	0	0	0
P	100	50	48.64	17.64	0	0	0	0
O	0	0	0	0	0	0	59.16	0
K	0	0	0	0	0	0	0	43.19

Table 4. Accuracy Assessment at 2m Resolution

Class	*AM*	*RA*	*RM*	*SA*	*T*	*U*	*O*	*K*
AM	30	12	11	25	78	38.46	0	0
RA	0	18	0	2	20	90	0	0
RM	0	0	19	0	19	100	0	0
SA	0	0	0	3	3	100	0	0
T	30	30	30	30	120	0	0	0
P	100	60	63.33	10	0	0	0	0
O	0	0	0	0	0	0	58.34	0
K	0	0	0	0	0	0	0	44.45

Table 5. Accuracy Assessment at 5m Resolution

Class	*AM*	*RA*	*RM*	*SA*	*T*	*U*	*O*	*K*
AM	40	17	14	6	77	51.95	0	0
RA	0	18	1	2	21	85.71	0	0
RM	0	0	18	0	18	100	0	0
SA	0	0	1	3	4	75	0	0
T	40	35	34	11	120	0	0	0
P	100	51.43	52.95	10	0	0	0	0
O	0	0	0	0	0	0	65.84	0
K	0	0	0	0	0	0	0	50.45

Table 6. Accuracy Assessment at 10m Resolution

Class	*AM*	*RA*	*RM*	*SA*	*T*	*U*	*O*	*K*
AM	45	18	7	7	77	58.45	0	0
RA	1	22	0	0	23	95.65	0	0
RM	2	0	14	0	16	87.5	0	0
SA	1	0	0	3	4	75	0	0
T	49	40	21	10	120	0	0	0
P	91.83	55	66.67	30	0	0	0	0
O	0	0	0	0	0	0	70	0
K	0	0	0	0	0	0	0	53.7

Table 7. Accuracy Assessment at 20m Resolution

Class	*AM*	*RA*	*RM*	*SA*	*T*	*U*	*O*	*K*
AM	51	15	6	5	77	66.24	0	0
RA	1	21	0	0	22	95.45	0	0
RM	3	0	15	0	18	83.34	0	0
SA	1	0	0	2	3	66.67	0	0
T	56	36	21	7	120	0	0	0
P	91.07	58.34	71.43	28.57	0	0	0	0
O	0	0	0	0	0	0	74.17	0
K	0	0	0	0	0	0	0	58.19

Table 8. Accuracy Assessment at 30m Resolution

Class	*AM*	*RA*	*RM*	*SA*	*T*	*U*	*O*	*K*
AM	50	14	5	2	71	70.42	0	0
RA	1	22	2	1	26	84.61	0	0
RM	1	1	16	0	18	88.89	0	0
SA	3	0	0	2	5	40	0	0
T	55	37	23	5	120	0	0	0
P	90.9	59.45	69.56	40	0	0	0	0
O	0	0	0	0	0	0	75	0
K	0	0	0	0	0	0	0	60.41

Table 9. Accuracy Assessment at 50m Resolution

Class	*AM*	*RA*	*RM*	*SA*	*T*	*U*	*O*	*K*
AM	53	18	5	0	76	69.73	0	0
RA	1	22	0	0	23	95.65	0	0
RM	1	2	14	0	17	82.35	0	0
SA	2	1	1	0	4	0	0	0
T	57	43	20	0	120	0	0	0
P	92.98	51.16	70	0	0	0	0	0
O	0	0	0	0	0	0	74.16	0
K	0	0	0	0	0	0	0	57.43

Table 3-9 presents the accuracy metrics for the following mangrove species: Avicennia Marina (AM), Rhizophora Apiculata (RA), Rhizophora Mucronata (RM), and Sonneratia Alba (SA). The abbreviations T, U, P, O, and K denote total, user accuracy, producer accuracy, overall accuracy, and kappa accuracy, respectively.

IV. CONCLUSION

The application of LSU based on spectral libraries on WorldView-2 imagery is effective for mapping mangrove species along the East Coast of Surabaya. High resolution (0.5–10 m) provides more detailed mapping but is more optimal for species with small and scattered distributions. Meanwhile, low resolution (20–50 m) tends to cause overestimation or aggregation of species. Based on the results of the LSU analysis based on spectral libraries on WorldView-2 imagery in the protected area of the East Coast of Surabaya, it shows that Avicennia Marina (AM) remains dominant and stable at all resolutions. Rhizophora Apiculata (RA) and Rhizophora Mucronata (RM) increase at lower resolutions, while Sonneratia Alba (SA) decreases.

Comparison of the area of mangrove species at various levels of WorldView-2 image resolution in the East Coast of Surabaya area shows that changes in image resolution significantly affect the estimated area of each species. Avicennia marina experienced an increase in area from 70.19 km² (37.46%) at 0.5 meter resolution to 70.97 km² (36.94%) at 50 meter resolution, while Rhizophora apiculata increased more significantly from 51.35 km² (27.39%) to 56.97 km² (29.66%). Rhizophora mucronata showed a fluctuating or inconsistent pattern, with the lowest area of 33.10 km² at 10 meter resolution and the highest of 40.37 km² (21.02%) at 50 meter resolution, indicating high sensitivity to changes in resolution and potential misclassification with other species. In contrast, Sonneratia alba experienced a decrease in area from 29.20 km² (15.58%) at 0.5 meter resolution to 23.77 km² (12.38%) at 50 meter resolution, indicating that this species is difficult to detect at coarse pixels due to its scattered and less dominant distribution.

LSU analysis yielded RMSE values indicating that AM, RA, and RM had low error values (≤ 0.5), while SA had RMSE > 0.5, indicating lower LSU accuracy in detecting these species, possibly due to their lower abundance. Therefore, LSU performed optimally at medium resolution (10–30 m), with overall accuracy increasing from 70% (10 m) to 75% (30 m) and Kappa values increasing from 53.7 to 60.41. To improve species differentiation, future studies can integrate additional spectral indices and explore advanced classification techniques, such as multi-resolution segmentation or hybrid machine learning approaches.

ACKNOWLEDGMENTS

The authors are grateful to the Technical Implementation Unit of the Surabaya Mangrove Botanical Garden for the assistance in supplying information related to mangrove species. This study was funded by Higher Education for Technology and Innovation ADB Loan No. 4110-INO ITS 2023 (contract number 0009/01.PKS/PPK-HETI/ITS/2023).

REFERENCES

[1] S. Abdul Azeez *et al.*, "Multi-decadal changes of mangrove forest and its response to the tidal dynamics of thane creek, Mumbai," *J Sea Res*, vol. 180, Feb. 2022, doi: 10.1016/j.seares.2021.102162.

[2] T. V. Tran, R. Reef, X. Zhu, and A. Gunn, "Characterising the distribution of mangroves along the southern coast of Vietnam using multi-spectral indices and a deep learning model," *Science of the Total Environment*, vol. 923, May 2024, doi: 10.1016/j.scitotenv.2024.171367.

[3] J. B. Thayn, "Monitoring Narrow Mangrove Stands in Baja California Sur, Mexico Using Linear Spectral Unmixing," *Marine Geodesy*, vol. 43, no. 5, pp. 493–508, Sep. 2020, doi: 10.1080/01490419.2020.1751753.

[4] P. J. Mumby *et al.*, "Mangroves enhance the biomass of coral reef fish communities in the Caribbean," *Nature*, vol. 427, no. 6974, pp. 533–536, Feb. 2004, doi: 10.1038/nature02286.

[5] E. B. Barbier, S. D. Hacker, C. Kennedy, E. W. Koch, A. C. Stier, and B. R. Silliman, "The value of estuarine and coastal ecosystem services," May 2011. doi: 10.1890/10-1510.1.

[6] Rahman *et al.*, "Mangrove ecosystems in Southeast Asia region: Mangrove extent, blue carbon potential and CO2 emissions in 1996–2020," *Science of The Total Environment*, vol. 915, p. 170052, Mar. 2024, doi: 10.1016/j.scitotenv.2024.170052.

[7] L. M. Jaelani *et al.*, "Mapping Mangrove Species Distribution and Density Using Sentinel-2 Satellite Imagery and Spectral Analysis," *Journal of Human, Earth, and Future*, vol. 6, no. 1, pp. 1–11, Mar. 2025, doi: 10.28991/HEF-2025-06-01-01.

[8] W. A. Timisela, G. Mardiatmoko, and F. Puturuhu, "ANALISA JENIS MANGROVE MENGGUNAKAN CITRA UAV DENGAN KLASIFIKASI OBIA," *JURNAL HUTAN PULAU-PULAU KECIL*, vol. 4, no. 2, pp. 132–149, Oct. 2020, doi: 10.30598/jhppk.2020.4.2.132.

[9] R. Asy'Ari *et al.*, "Mapping mangrove forest distribution on Banten, Jakarta, and West Java Ecotone Zone from Sentinel-2-derived indices using cloud computing based Random Forest," *Jurnal Pengelolaan Sumberdaya Alam dan Lingkungan (Journal of Natural Resources and Environmental Management)*, vol. 12, no. 1, pp. 97–111, May 2022, doi: 10.29244/jpsl.12.1.97-111.

[10] M. F. Hidayatullah, M. Kamal, and P. Wicaksono, "Geographic Object-Based Image Analysis for Mangrove Species Distribution Mapping," 2023, pp. 207–210. doi: 10.1007/978-3-031-43169-2_43.

[11] M. K. Heenkenda, K. E. Joyce, S. W. Maier, and R. Bartolo, "Mangrove species identification: Comparing WorldView-2 with aerial photographs," *Remote Sens (Basel)*, vol. 6, no. 7, pp. 6064–6088, 2014, doi: 10.3390/rs6076064.

[12] N. Patidar and A. K. Keshari, "A rule-based spectral unmixing algorithm for extracting annual time series of sub-pixel impervious surface fraction," *Int J Remote Sens*, vol. 41, no. 10, pp. 3970–3992, May 2020, doi: 10.1080/01431161.2019.1711243.

[13] Y. Zhang, T. Wang, S. Mei, and Q. Du, "Subpixel Mapping of Hyperspectral Images Using a Labeled-Unlabeled Hybrid Endmember Library and Abundance Optimization," *IEEE J Sel Top Appl Earth Obs Remote Sens*, vol. 13, pp. 5036–5047, 2020, doi: 10.1109/JSTARS.2020.3012982.

[14] L. Breiman, "Random Forests," *Mach Learn*, vol. 45, no. 1, pp. 5–32, Oct. 2001, doi: 10.1023/A:1010933404324.

[15] A. N. Alina, M. A. Syariz, L. M. Jaelani, and N. Hayati, "Accuracy Results Comparison of Machine Learning Classification for Mangroves on Worldview-2 Satellite Imagery," 2024.

[16] R. Rajabi and H. Ghassemian, "Sparsity Constrained Graph Regularized NMF for Spectral Unmixing of Hyperspectral Data," *Journal of the Indian Society of Remote Sensing*, vol. 43, no. 2, pp. 269–278, Jun. 2015, doi: 10.1007/s12524-014-0408-2.

[17] N. Keshava and J. F. Mustard, "Spectral unmixing," *IEEE Signal Process Mag*, vol. 19, no. 1, pp. 44–57, 2002, doi: 10.1109/79.974727.

[18] L. M. Jaelani, R. Limehuwey, N. Kurniadin, A. Pamungkas, E. S. Koenhardono, and A. Sulisetyono, "Estimation of TSS and Chl-a Concentration from Landsat 8-OLI: The Effect of Atmosphere and Retrieval Algorithm," 2016. [Online]. Available: http://espa.cr.usgs.gov/

[19] M. M. R. Devy, H. Sanjaya, L. Y. Irawan, I. K. Astina, H. Sadmono, and A. Andayani, "Large-Extent Mangrove Species Mapping Using Landsat 9 OLI-2: A Subpixel Analysis," in *2022 IEEE Asia-Pacific Conference on Geoscience, Electronics and Remote Sensing Technology: Understanding the Interaction of Land, Ocean, and Atmosphere: Smart City and Disaster Mitigation for Regional Resilience, AGERS 2022 - Proceeding*, Institute of Electrical and Electronics Engineers Inc., 2022, pp. 130–136. doi: 10.1109/AGERS56232.2022.10093313.

[20] G. M. Foody, "Explaining the unsuitability of the kappa coefficient in the assessment and comparison of the accuracy of thematic maps obtained by image classification," *Remote Sens Environ*, vol. 239, no. December 2019, p. 111630, 2020, doi: 10.1016/j.rse.2019.111630.

[21] D. A. Roberts, M. Gardner, R. Church, S. Ustin, G. Scheer, and R. O. Green, "Mapping chaparral in the Santa Monica Mountains using multiple endmember spectral mixture models," *Remote Sens Environ*, vol. 65, no. 3, 1998, doi: 10.1016/S0034-4257(98)00037-6.

[22] A. Géron, *Hands-on Machine Learning with Scikit-Learn, Keras, and TensorFlow, 2nd edition (2019, O'reilly)*. O'Reilly Media, 2019.

[23] N. M. Short, "The Landsat tutorial workbook: basics of satellite remote sensing.," 1982, doi: 10.2307/635039.

[24] J. R. Jensen and K. Lulla, "Introductory digital image processing: A remote sensing perspective," *Geocarto*

Int, vol. 2, no. 1, p. 65, 1987, doi: 10.1080/10106048709354084.

[25] M. M. R. Devy, H. Sanjaya, L. Y. Irawan, I. K. Astina, H. Sadmono, and A. Andayani, "Large-Extent Mangrove Species Mapping Using Landsat 9 OLI-2: A Subpixel Analysis," in *2022 IEEE Asia-Pacific Conference on Geoscience, Electronics and Remote Sensing Technology: Understanding the Interaction of Land, Ocean, and Atmosphere: Smart City and Disaster Mitigation for Regional Resilience, AGERS 2022 - Proceeding*, Institute of Electrical and Electronics Engineers Inc., 2022, pp. 130–136. doi: 10.1109/AGERS56232.2022.10093313.